PALYNOLOGY
2018, VOL. 42, NO. S1, 93–110
https://doi.org/10.1080/01916122.2018.1465735

Taxonomic re-investigation and geochemical characterization of Reid's (1974) species of *Spiniferites* from holotype and topotype material

Pieter R. Gurdebeke[a], Kenneth Neil Mertens[a,b], Kara Bogus[c,d], Fabienne Marret[e], Nicolas Chomérat[b], Henk Vrielinck[f] and Stephen Louwye[a]

[a]Department of Geology, Ghent University, Gent, Belgium; [b]Ifremer, LER BO, Station de Biologie Marine, Concarneau Cedex, France; [c]Centre for Environmental Geochemistry, School of Geography, University of Nottingham, Nottingham, UK; [d]International Ocean Discovery Program, Texas A&M University, College Station, TX, USA; [e]School of Environmental Sciences, University of Liverpool, Liverpool, UK; [f]Department of Solid State Sciences, Ghent University, Gent, Belgium

ABSTRACT

The genus *Spiniferites* currently encompasses 142 dinoflagellate cyst species. Some *Spiniferites* species are difficult to identify because of an incomplete or doubtful description, and/or substandard iconography. This study re-describes and re-illustrates the *Spiniferites* holotypes first described by Reid in 1974. It also discusses topotype material from surface sediments recovered from British estuaries, and attempts to provide further constraints on the classification of species in this genus using the geochemical characterization of their cyst walls. Reid described four new *Spiniferites* species: *Spiniferites belerius*, *Spiniferites delicatus*, *Spiniferites elongatus* and *Spiniferites lazus*. New photomicrographs are presented here for the holotypes of *Spiniferites delicatus* and *Spiniferites elongatus*, and additional morphological observations based on newly processed topotype material are given. The geochemical characterization of the *Spiniferites* cyst walls showed overall consistency with a carbohydrate-based dinosporin. However, variability in the dinosporins suggests that, in this genus, the cyst wall composition may be species-specific. Analysis of the characteristic spectral regions for unclassified *Spiniferites* species showed that, in some cases, it may be possible to constrain the likely species affinity using the cyst wall chemistry. However, in most cases, the morphologically unspeciated cysts did not show sufficient similarity to an identified species' cyst wall chemistry to be more conclusive. This could either reflect an intermediate species that cannot be clearly characterized using morphology or dinosporin composition, or it represents a completely different species. In either case, both the morphological and geochemical evaluations highlight the difficulties in classifying species of this genus unequivocally.

KEYWORDS

Dinoflagellate cyst; redescription; taxonomy; geochemistry; cyst wall composition; FTIR; dinosporin

1. Introduction

The genus *Spiniferites* Mantell 1850, currently encompassing 142 species (Fensome et al. 2008), is renowned for the difficulty in distinguishing different species, often with species morphology intergrading between each other (Mertens et al. 2018). Furthermore, the cyst-theca relationship of many species remains unclear (e.g., Rochon et al. 2009).

Reid (1972, 1974, 1977) studied dinoflagellate cyst assemblages from estuaries around the British Isles (Figure 1). The assemblages were recovered from surface sediments and included 11 species belonging to the genus *Spiniferites* (Mantell 1850). Four species were considered new to science and formally described in Reid (1974): *Spiniferites belerius*, *Spiniferites delicatus*, *Spiniferites elongatus* and *Spiniferites lazus*. The other *Spiniferites* species recovered and documented by Reid (1974) included *Spiniferites bentorii* (Rossignol 1964) Wall and Dale 1970, *Spiniferites bulloideus* (Deflandre and Cookson 1955) Sarjeant 1970, *Spiniferites hyperacanthus* (Deflandre and Cookson 1955) Cookson and Eisenack 1974, *Spiniferites membranaceus* (Rossignol 1964) Sarjeant 1970, *Spiniferites mirabilis* (Rossignol 1964) Sarjeant 1970, *Spiniferites pachydermus* (Rossignol 1964) Reid 1974 and *Spiniferites ramuliferus* (Deflandre 1937) Reid 1974. Reid (1974) transferred the latter species from *Achomosphaera*, and it is now considered synonymous with *Achomosphaera ramosasimilis* (see Mertens et al. 2018). In this study, the holotypes of two of the four new *Spiniferites* species defined by Reid (1974), *Spiniferites delicatus* and *Spiniferites elongatus*, were re-examined and re-photographed. Newly processed sediment samples from topotype localities allowed further observations to elucidate the morphology of the species and document them with new photomicrographs.

In addition to the taxonomic re-evaluation, the composition of several *Spiniferites* species' cyst walls, including three of the species described by Reid (1974), *Spiniferites belerius*, *Spiniferites delicatus*, and *Spiniferites elongatus*, were measured and analyzed using micro-Fourier transform infrared (FTIR) spectroscopy. Micro-FTIR is a widely used technique for the evaluation of biopolymers (Olcott-Marshall and

CONTACT Pieter R. Gurdebeke pieter.gurdebeke@ugent.be Department of Geology, Ghent University, Krijgslaan 281, S8, B-9000 Gent, Belgium
Color versions of one or more of the figures in the article can be found online at www.tandfonline.com/tpal.

Published online 14 Dec 2018

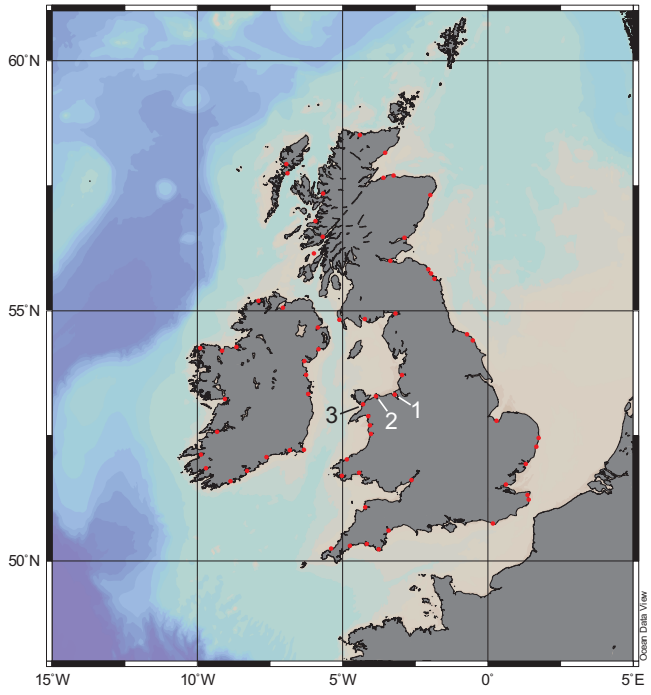

Figure 1. Location of the samples studied by Reid (1974) (red dots). Topotype localities from the Irish Sea are indicated as 1 (Dee estuary), 2 (Conwy Marina) and 3 (Caernarvon).

Marshall 2015, and references therein) and has been successfully used in the geochemical analysis of both fossil (e.g., Versteegh et al. 2007, Bogus et al. 2012) and recent (e.g., Kokinos et al. 1998; Versteegh et al. 2012; Bogus et al. 2014; Mertens et al. 2015a, 2015b, 2018) dinoflagellate cysts.

Dinoflagellate cyst walls are composed of dinosporin, suggested to be a complex carbohydrate-based biomacromolecule. Dinosporin was initially described as such based on FTIR and pyrolysis gas chromatography-mass spectrometry of *Lingulodinium machaerophorum* from culture and surface sediments (Versteegh et al. 2012); additional analyses suggested that considerable differences in composition between species of the same genus are possible (Bogus et al. 2012). Thus, it appears phylogeny could be a factor contributing to dinosporin compositional differences. However, this suggestion is limited by the fact that species from different genera, environmental conditions (surface waters and post-depositional) and regions have primarily been compared (e.g., Bogus et al. 2014). These other factors seemingly influence the dinosporin composition (e.g., Bogus et al. 2014; Mertens et al. 2015a, 2015b, 2017), a finding consistent with the fact that dinoflagellate cyst morphology as well can vary with differing environmental conditions (e.g., Ellegaard 2000; Lewis et al. 2001; Ellegaard et al. 2002; Zonneveld and Susek 2007; Mertens et al. 2009).

By comparing the cyst wall chemistry of *Spiniferites* species from the same location (Dee Estuary), likely deposited at about the same time, we can constrain most of these uncertainties. This allowed us to investigate the extent to which a particular dinosporin composition may be species specific. Our results were then used in an attempt to constrain the speciation of specimens that could not be visually assigned because of unclear morphology.

2. Material and methods

2.1. Observation of holotypes and topotypes

The holotypes of *Spiniferites belerius*, *Spiniferites delicatus*, *Spiniferites elongatus* and *Spiniferites lazus* are stored in the repository at the Micropalaeontology Laboratory, Geology Department of the University of Sheffield (UK) under catalogue numbers 69K1 1331.568(4), 12 ABSL1 1290.192(5), 140 K3 1210.352(12) and 73K1 1365.256(2), respectively. These specimens were re-examined by P.R.G. during summer 2014.

Topotype material was sampled in the Dee, Caernarvon and Conwy Marina estuaries (Figure 1). The saltmarsh surface sediment was carefully hand-collected in a 50 ml plastic tube that was covered with black tape. All samples were then kept in the dark, at 4 °C. Additional samples were investigated from previously studied surface samples from the Celtic Sea (location details in Marret et al. 2004) and surface samples from Britanny (Vilaine Estuary, location details in Mertens et al. 2009). The palynological processing of the topotype and additional samples followed the procedure described by e.g., Pospelova et al. (2010). Samples were treated with 10% hydrochloric acid (HCl) at room temperature to remove carbonates. After rinsing with distilled water, samples were treated with hydrofluoric acid (HF, 48-50%, 2 days) to remove silicates, followed by a second 10% HCl treatment to remove precipitated fluorosilicates. The samples were rinsed again and sonicated up to 30 seconds and the residue was sieved and retained on a nylon mesh screen (15 μm). One or two drops of the residue were mounted on a slide with glycerine jelly and covered with a cover slip.

The holotypes were photographed at the University of Sheffield with an Infinity 1 camera mounted on a Meiji MT 5300H microscope, while the specimens from the topotype material were photographed at a 100× magnification with an MRc5 camera mounted on a Zeiss Axio Imager A1 at Ghent University and with an Olympus DP72 camera mounted on a BX41 microscope at the Station de Biologie Marine (Ifremer, Concarneau). For scanning electron microscope (SEM) observations, single cysts were picked from the residue and mounted on a glass slide or were filtered using polycarbonate membrane filters (Millipore, Billerica, MA, USA, GTTP Isopore, 0.22 μm pore size), sputter coated with gold, and examined using a JEOL6400 SEM at Ghent University and a Zeiss SIGMA300 Gemini field emission SEM at the Station de Biologie Marine (Ifremer, Concarneau).

The holotypes of *Spiniferites delicatus* and *Spiniferites elongatus* were successfully identified in the palynological collections at the University of Sheffield. The holotypes of *Spiniferites belerius* and *Spiniferites lazus* were not found due to the poor condition of the slides. All of the *Spiniferites* species identified by Reid (1974), except *Spiniferites bentorii*, *Spiniferites hyperacanthus* and *Spiniferites pachydermus*, were found in the newly processed samples from topotype localities.

Additional observations, for illustrative purposes, of '*Spiniferites ramuliferus*' were made on residues from the type stratum and locality of *Spiniferites coniconcavus* in the

Pliocene Verrebroek Dock section in Belgium (processing details in De Schepper et al. 2004).

2.2. Geochemical analysis of cyst wall chemistry

The palynological residues from topotype material (Dee Estuary) were then treated for geochemical analysis. They were sonicated and rinsed three times with organic solvents (methanol and dichloromethane) and water to remove polar and apolar compounds that might have adhered to the outside of the cyst walls. Visually clean individual cysts were manually isolated, placed on an Au-coated mirror and dried. Specimens were analyzed with a Bruker Hyperion 2000 microscope coupled to a Bruker Vertex 80v FTIR spectrometer at the Department of Solid State Sciences (Ghent University). Magnification of the microscope was set at 15x and the aperture adapted to the size of the measured specimen. The combination of detector (liquid N_2 cooled MCT detector), source (Globar) and beamsplitter (KBr) settings restrict the infrared spectral range examined to ~7000–600 cm^{-1}, from these spectra the 4000–650 cm^{-1} range was selected for analysis in this study. All presented spectra were collected in reflection mode, at a resolution of 2 cm^{-1} and averaged over 100 scans.

Data were analyzed with the OPUS software. The presented absorbance spectra were obtained after background (direct reflection on the Au mirror) subtraction and baseline correction (rubberband correction method using polynomes and 5 iterations). Residual CO_2 absorption traces at ~2350 cm^{-1}, a result of incomplete N_2 gas purging of the microscope, have also been removed. Functional groups were identified based on comparison with published literature. Relative strengths of the main IR band regions within a specimen's spectrum were calculated by integrating the area under the peaks between defined band limits to allow comparisons between spectra. The ranges of these IR bands are: (I) 3010–2775 cm^{-1}, (II) 1850–1500 cm^{-1}, (III) 1500–1185 cm^{-1}, (IV) 1185–860 cm^{-1}.

3. Systematic paleontology

Division DINOFLAGELLATA (Bütschli 1885) Fensome et al. 1993, emend. Adl et al. 2005

Class DINOPHYCEAE Pascher 1914

Subclass PERIDINIPHYCIDAE Fensome et al. 1993

Order GONYAULACALES Taylor 1980

Suborder Gonyaulacineae autonym

Family Gonyaulacaceae Lindemann 1928

Subfamily Gonyaulacoideae autonym

Genus *Spiniferites* Mantell 1850, emend. Sarjeant 1970

Spiniferites belerius Reid 1974

Plate 3, Figures 1–12.

Synonymy. non *Spiniferites belerius* in Harland 1977, p. 98–99, Plate 1, Figures 7–10, Plate 2, figures 7–10, 16–21, 25–57 [these images correspond to *Spiniferites membranaceus*; Harland (1979) also reports *Spiniferites belerius* from the Pliocene and Pleistocene of the Bay of Biscay, but does not provide photographs; the confirmation of a correct identification in that paper can thus not be given].

Dimensions. Reid (1974) – holotype: central body: 35–29 μm; length processes: 10 μm. Range: length central body: 35–42 μm; width central body: 28–37 μm; depth 33–37 μm. Maximum process length: 7–10 μm; maximum posterior process length: 10–15 μm. Number of specimens measured: 15.

Our measurements on topotype material from the Dee, Conwy Marina and Caernarvon estuaries – central body length 32 (34.8) 38 μm; width 27.6 (30.2) 32 μm; process length 6.4 (8.3) 11 μm. Number of specimens measured: 7. These new measurements are comparable with those described by Reid (1974) although somewhat in the lower part of the range. This is similar to the measurements reported by Harland (1977).

Original description (Reid 1974, p. 597). "Test oval, always widest at the girdle; at times constricted towards the poles to give a rounded diamond shape with a clear apical node. The thin smooth surfaced wall is ornamented by gonal trifurcate processes formed from sutural septae. Septae form the high antapical 'trumpet' shaped process which characterizes the species and may also form high membranous flanges. Process tips are trifurcate with recurved bifurcate tips. A relatively narrow 6–8 μm girdle is displaced by one to three times its own width."

Additional observations. Typically, these cysts are the smallest *Spiniferites* species in the assemblages. The cysts are ovoid with a very finely granular wall (both endophragm and periphragm) (Plate 3, Figure 12). A small apical boss is present (Plate 3, Figure 10). Sutures reveal a tabulation typical for the genus of 4′, 6″,?c,?s, 6‴, 1p, 1⁗ (not reported by Reid 1974). The suture between 1′ and 4′ is faint but visible, while 6″ is triangular. The sulcal plates are faintly discernible, but we could not observe all of them. The archeopyle corresponds to plate 3″. The processes are rigid and hollow, and exclusively gonal. The distal ends of the processes are typically trifurcate, and each furcation terminates in bifurcate tips, which can be elongated or truncated (Plate 3, Figure 6). The bases of the processes are wide (7.1 μm on average). Reid (1974) defined *Spiniferites belerius* as characterized by an antapical trumpet-shaped process located at the junction of the 1″ and 2‴ plates (i.e. an antapical position). We assume Reid meant the large box-like process we observed at the junction of plates 1⁗ and 1p (thus left of the sulcus) (Plate 3, Figure 3). We suggest it is formed by the fusion of two adjacent processes.

Comparison. *Spiniferites belerius* resembles *Spiniferites conicon-cavus* De Schepper et al. (2004) from the Pliocene of Belgium, but the latter lacks an apical boss (Pl. 10, Figures 1–3). *Spiniferites belerius* differs from "*Spiniferites bulloideus* sensu Wall 1965" in that *S. belerius* has an apical boss. Its differences with *Spiniferites bentorii* are the larger size, the pear-shaped body, the pronounced apical boss and the occurrence of fenestrate bases in *Spiniferites bentorii*. At this time the presence/absence of an apical boss is considered to vary interspecifically and intraspecifically and there is no conclusive evidence for its taxonomic importance (Mertens et al. 2018).

Remarks. The holotype was not located in the original slide, possibly because of the poor condition of the slide. The observed specimens were recorded from the Dee and Caernarvon estuaries and the Conwy Marina.

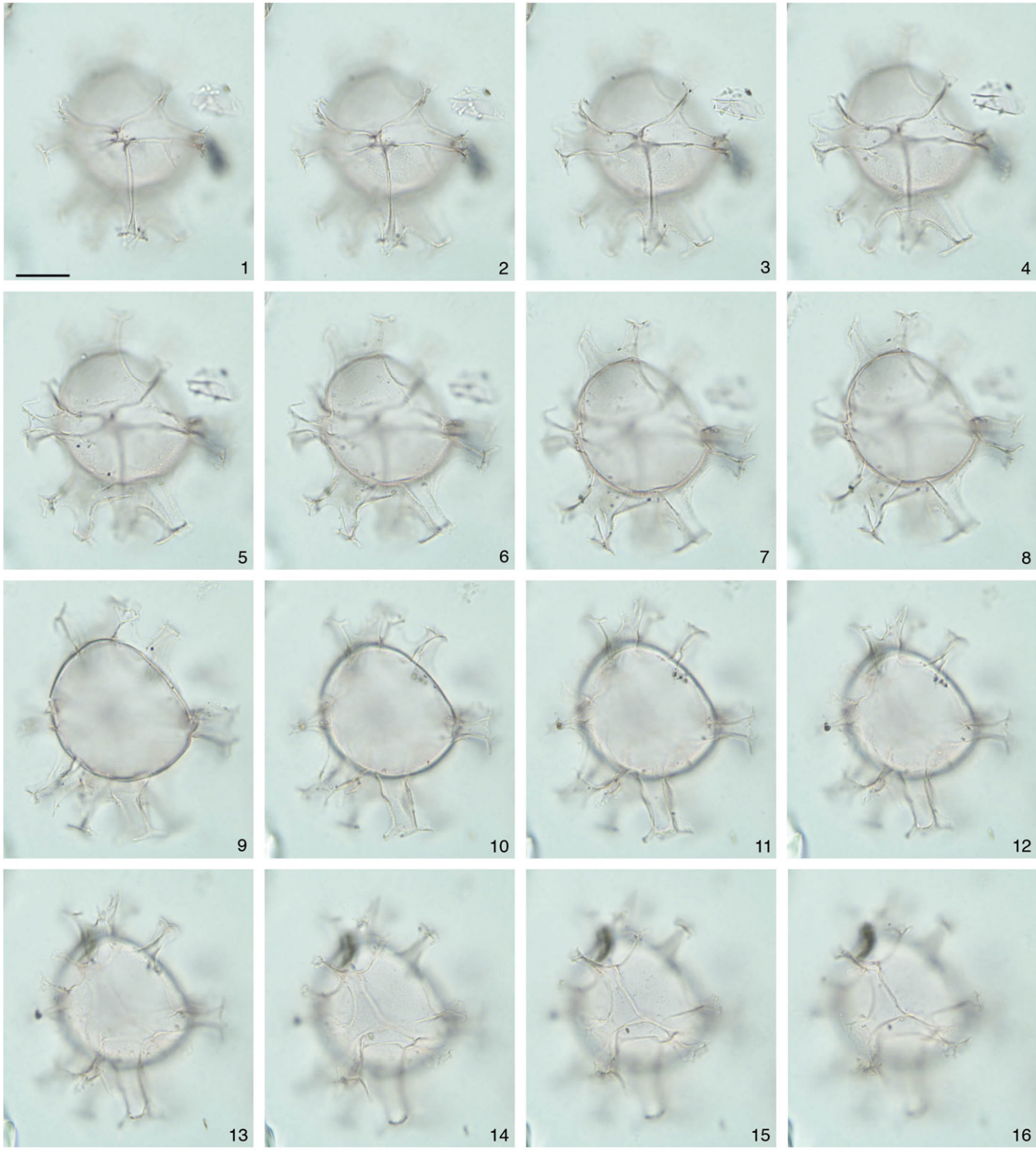

Plate 1. Figures 1–16: *Spiniferites delicatus*. Holotype 12 ABSL 1290.192(5). 1–7: High focus, incrementally lowering; 8–9: Optical sections; 10–16: Low focus, incrementally lowering. Scale bar =10 μm.

Occurrence. From the base of the Pliocene to Recent. Specimens recorded in older Neogene sediments are mentioned as *Spiniferites* cf. *belerius* (Londeix et al. 2018).

Spiniferites delicatus Reid 1974

Plate 1, Figures 1–16 (holotype), Plate 4, Figures 1–9.

Synonymy. None.

Dimensions. Reid (1974) – holotype: central body: 47 × 49 μm; length processes: 21 μm, width girdle: 7 μm. Range: central body: 40 × 35 to 60 × 54 μm. Maximum height processes: 29 μm; width girdle: 6–9 μm. Number of specimens measured: 18. Our measurements on topotype material from the Irish Sea – length 36.8 (41.5) 50.8 μm; width 40 (42) 46 μm. Number of specimens measured: 5.

Original description (Reid 1974, p.601). "The cyst wall is thick, with radial 'columellae' or fibres in the endophragm and with a much thinner granular periphragm. The surface is microgranular to microreticulate. Processes are supported by thin skeletal rods which trifurcate and then bifurcate in the

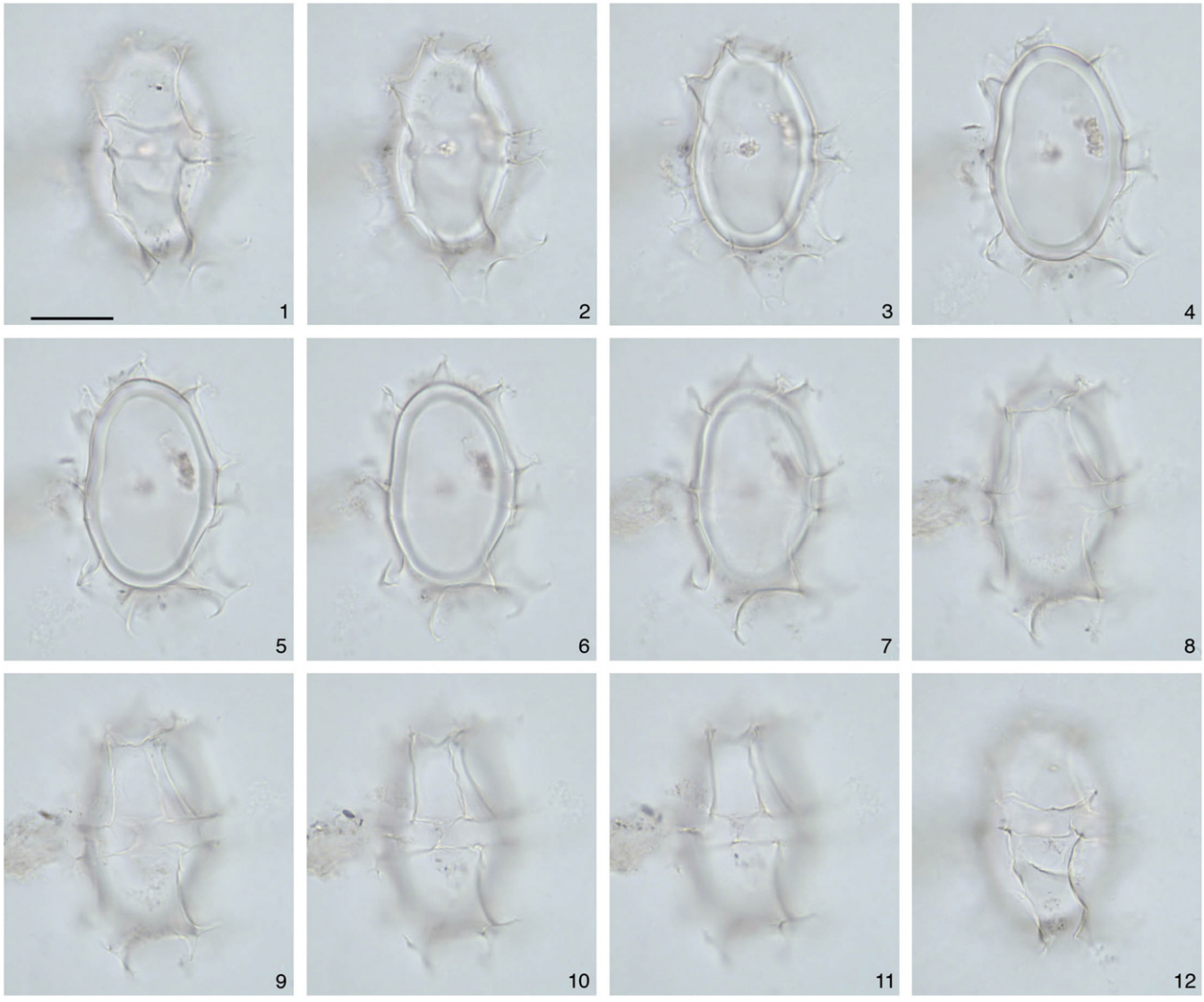

Plate 2. Fig. 1–12: *Spiniferites elongatus*. Holotype 140K3 1210.352(12). 1–3: High focus, incrementally lowering; 4-5: Optical sections; 6–12: Low focus, incrementally lowering. Scale bar =10 μm.

process tips. These processes are usually connected by high granular membranous flanges which vary greatly in their development in individual specimens. An apical node or low boss may be found at the head of 1′ and 4′. In most specimens the sutural flanges are of equal height over the whole test, but a few may have high antapical flanges surrounding 1′′′′. The girdle is sinistral and is displaced by three times its width. The sulcus which is orientated posterior/anteriorly [*sic*]. It has the following sulcal plates: PS, IS, LS, RA and AS. The tabulation is typical for the genus with an apical series of four plates and a precingular archeopyle 3′′ which is reduced."

Additional observations. The central body of the cyst is spherical to ovoidal. Our observations and measurements indicate that the central body of the specimens from the topotype material are mostly spherical, and somewhat smaller compared to the measurements of Reid (1974). The inner and outer walls are granular, closely appressed except at the base of the processes. The sutural crests are high, particularly on the antapical and cingular sides. The crests are granular and connect the exclusively gonal processes, which are also granular. The distal ends of the processes are consistently petaloid in plan view. Both processes and crests have faintly granular surfaces. The girdle is sinistral and is displaced by three times its width.

Comparison. *Spiniferites ristingensis* Head 2007 (Plate 9, Figures 1–8) has similar processes, but the wall appears to be thinner with a tegillum that forms blisters and lower sutural crests. The central body length of *Spiniferites ristingensis*, 39 (43.0) 49 μm, is slightly smaller than that of *Spiniferites delicatus*, as given by Reid (1974).

Remarks. The holotype from Reid (1974) is shown in Plate 1. Additional specimens were observed in topotype material from the estuaries around the Irish Sea (Conwy Marina, Dee, Caernarvon). There was overall agreement during the Second *Spiniferites* Workshop in Ostend in 2015 that the so-called "skeletal rods", first described by Reid (1974), do not exist and are an optical illusion created by the attachment of membranes along the processes (Mertens et al. 2018).

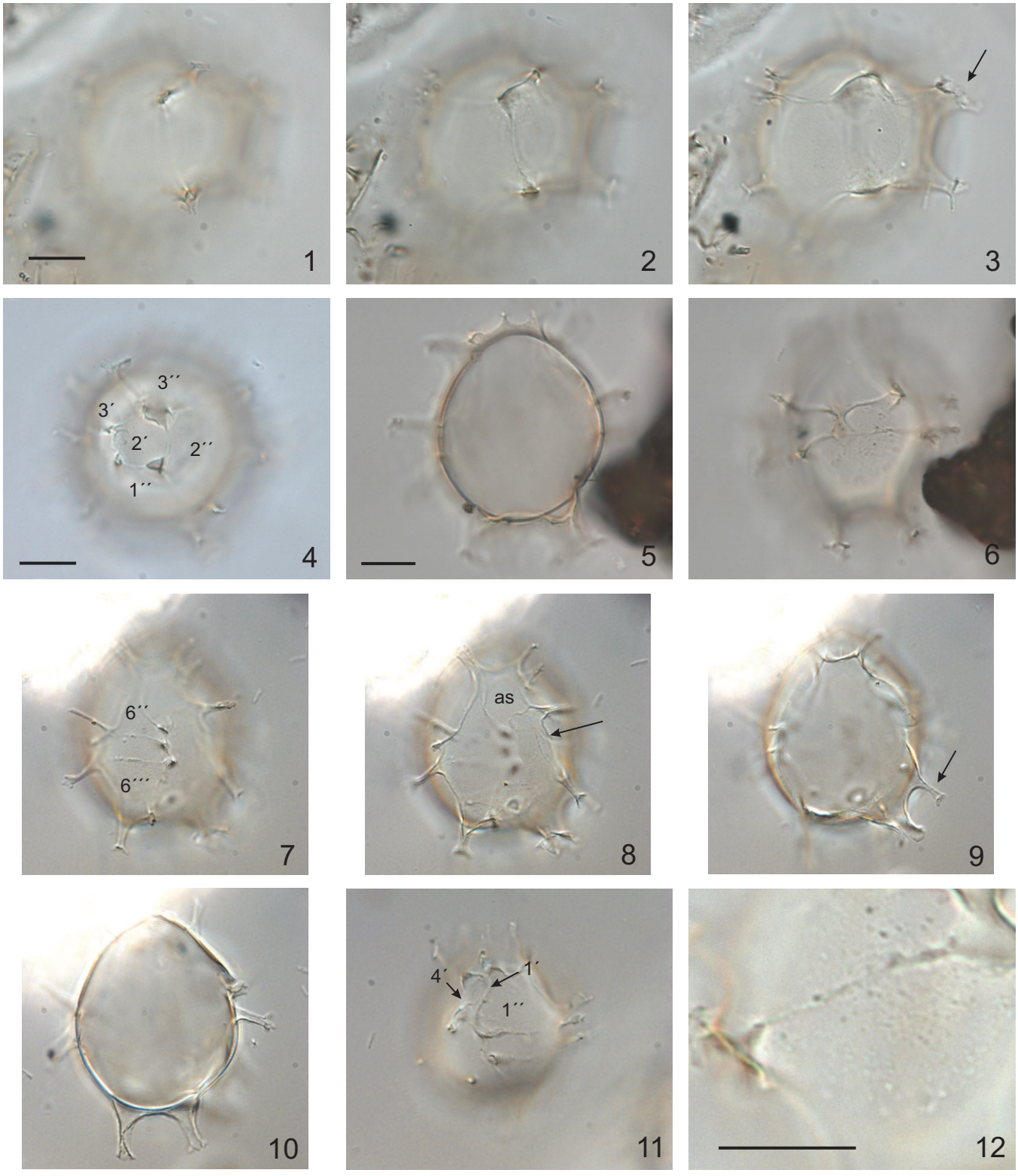

Plate 3. 1–12: *Spiniferites belerius*. 1–3: Dee Estuary slide 1/3 sp. 1, incrementally lowering focus. 4: Dee Estuary slide 1/3 sp. 2, high focus. 5–6: Dee Estuary slide 3/3; 5: optical section, 6: low focus. 7–10: Dee Estuary slide B/B sp. 1, incrementally lowering focus; 10: optical section. 11: Dee Estuary slide B/B sp. 2, high focus. 12: Dee Estuary l.l, detail of wall structure. Scale bar =10 μm.

Occurrence. From the lower Miocene onwards (Londeix et al. 2018).

Spiniferites elongatus Reid 1974

Plate 2, Figures 1–12 (holotype). Plate 5, Figures 1–6.

Synonymy. *Spiniferites ellipsoideus* Matsuoka 1983, see Mertens et al. 2018.

Dimensions. Reid (1974) – holotype: 30 × 49 μm; height antapical process: 13 μm; height apical process: 6 μm; height lateral process: 9 μm. Range: test 26 × 40 μm to 42 × 59 μm; height antapical processes: 12–16 μm; height apical processes: 6–12 μm; height lateral processes: 5–9 μm. Number of specimens measured: 15. Our measurements on topotype

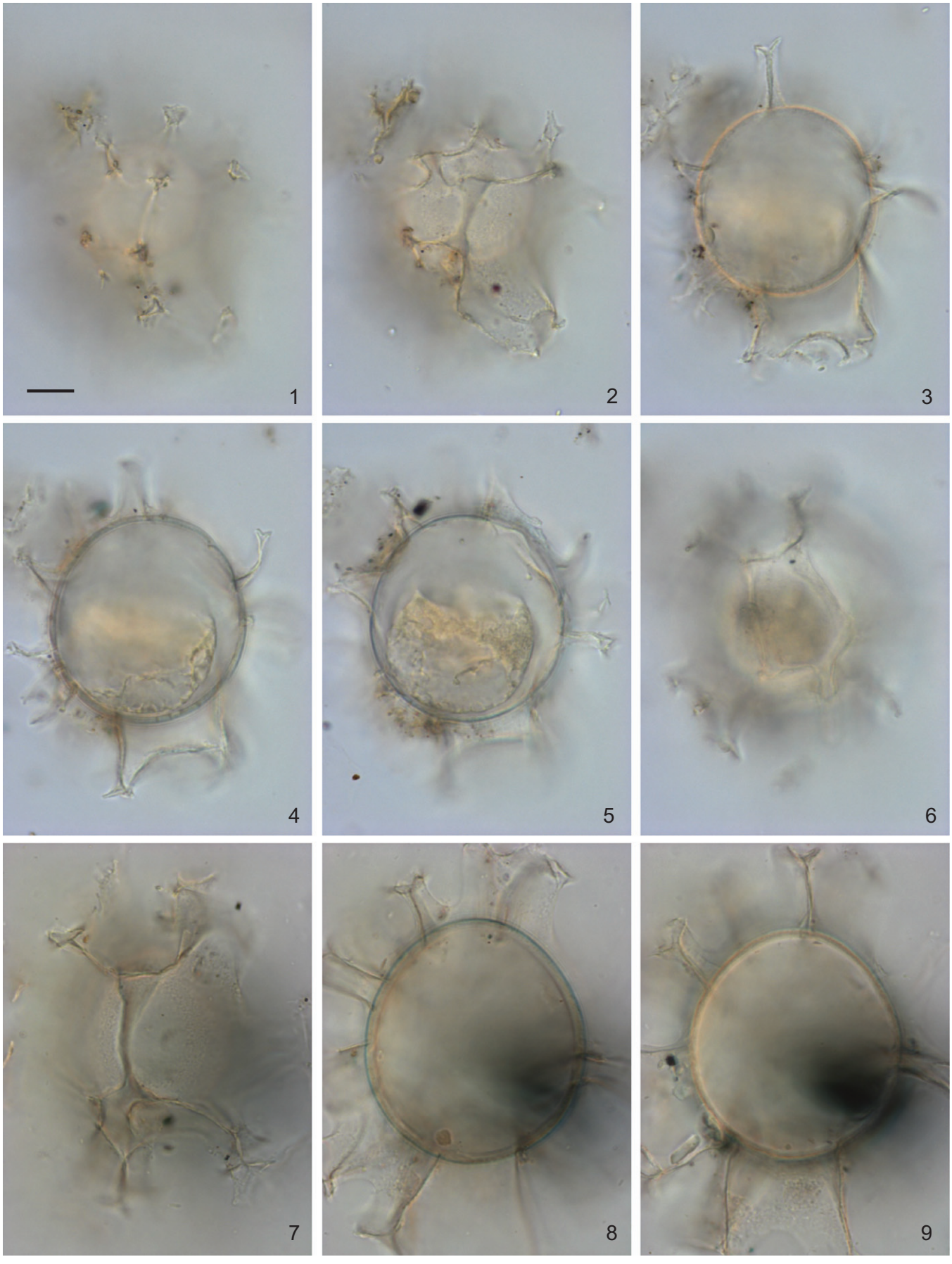

Plate 4. Fig. 1–9: *Spiniferites delicatus*. 1–6: Celtic Sea 9-8 St. 8 5100; 1–2 High focus, incrementally lowering; 3: Optical section; 4–6: Low focus, incrementally lowering. 7–9: Celtic Sea St. 8 11 1 99 0 cm cs 5–6; 7: High focus; 8: Optical section; 9: Low focus. Scale bar =10 μm.

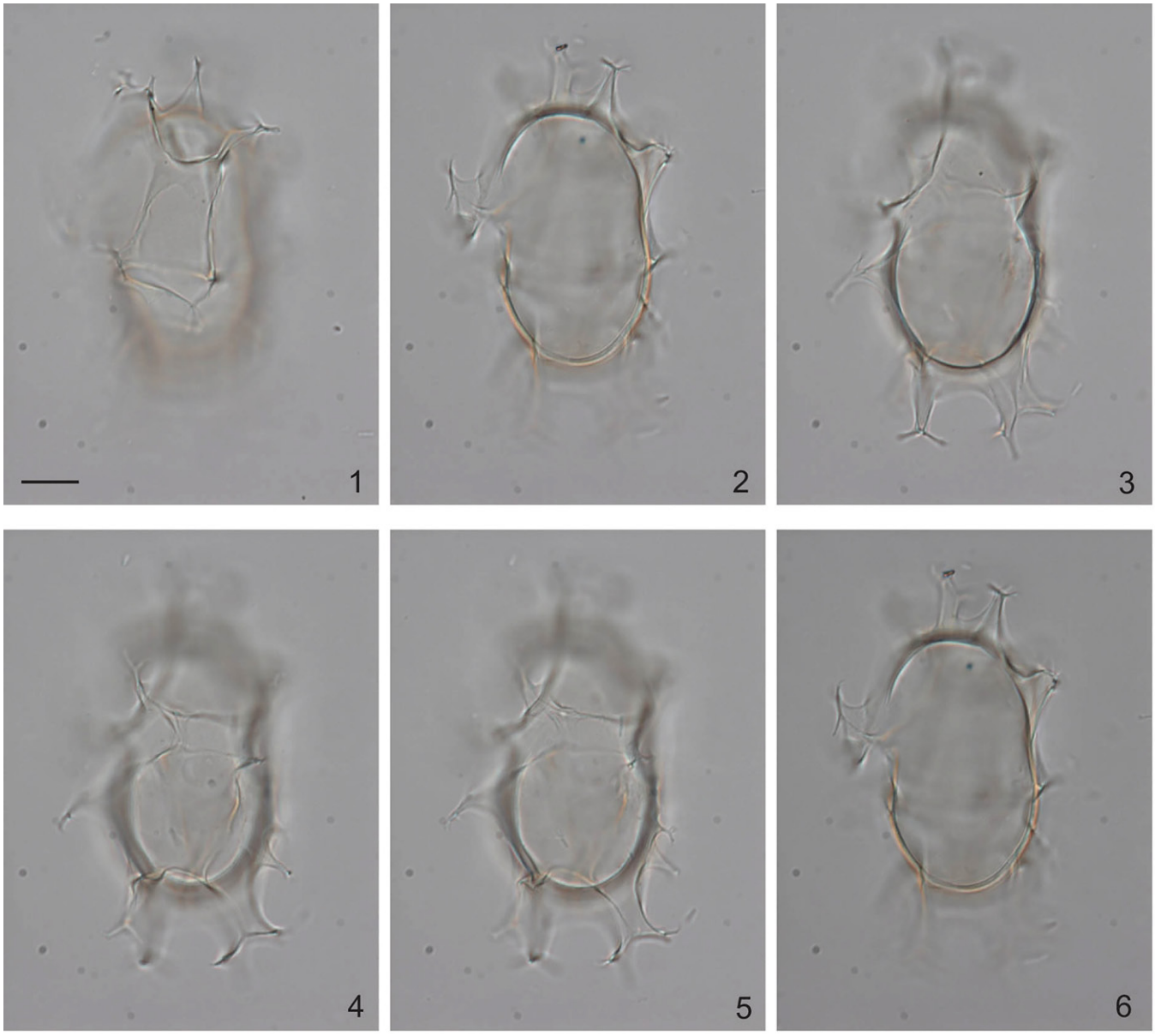

Plate 5. Fig. 1–6: *Spiniferites elongatus*. Dee estuary. 1: High focus; 2: Optical section; 3–6: Low focus, incrementally lowering. Scale bar =10 μm.

material from Dee Estuary – length 32 (38) 44 μm; width 20 (25) 30 μm. Number of specimens measured: 2.

Original description (Reid 1974, p. 603). "In polar view the test is circular. It has a thin, 0.8–1 μ wall with a smooth surface and no evidence of an apical boss. A short complex process is found at the head of the sulcus. At the junction of 1′′′′ and 3′′′ high membranous septae join two stout simple processes and at the junctions of 5′′′, 4′′′, 1′′′′ and 1P, 2′′′, 1′′′′ two high, hollow, trumpet shaped processes are found. Their multifurcate tips appear to be supported by strengthening rods. These are joined to each other and to the previous two simple processes by high septae. No sulcal plates were seen. Tabulation appears to be typical for the genus except for plate 1′′′ which is either absent or is covered by the wide septate of 2′′′ and 1P at the junction with the sulcus. Plates 1′ and 4′ are not fused but are separated by a low septa. Plate 6′′ is triangular, long and narrow. Archeopyle precingular 3′′ and reduced."

Additional observations. The cysts have an elongate or ellipsoidal ambitus, and are circular in polar view. The surface is smooth to finely microgranular and no apical boss was observed. Wide flaring sutural crests are attached towards the center of the plates and leave an oval impression in the center of each plate (Plate 2, Figure 8; Plate 5, Figure 1). At the antapex, the sutural crests are high (4 μm, see Plate 5, Figure 5) and connect complex processes. The sutural crests at the apex are high as well, but lower than on the antapex (Plate 5, Figure 2), while elsewhere on the cyst, the crests are lowest, and connect simple processes. Girdle displaced by less than its own width.

Comparison. All elongate specimens recorded in the newly processed samples are identified as *Spiniferites elongatus* and no other elongate species such as *Spiniferites frigidus* or *Rottnestia amphicavata* were recorded. The relation to these taxa as a single morphospecies is further discussed in Van Nieuwenhove et al. (2018).

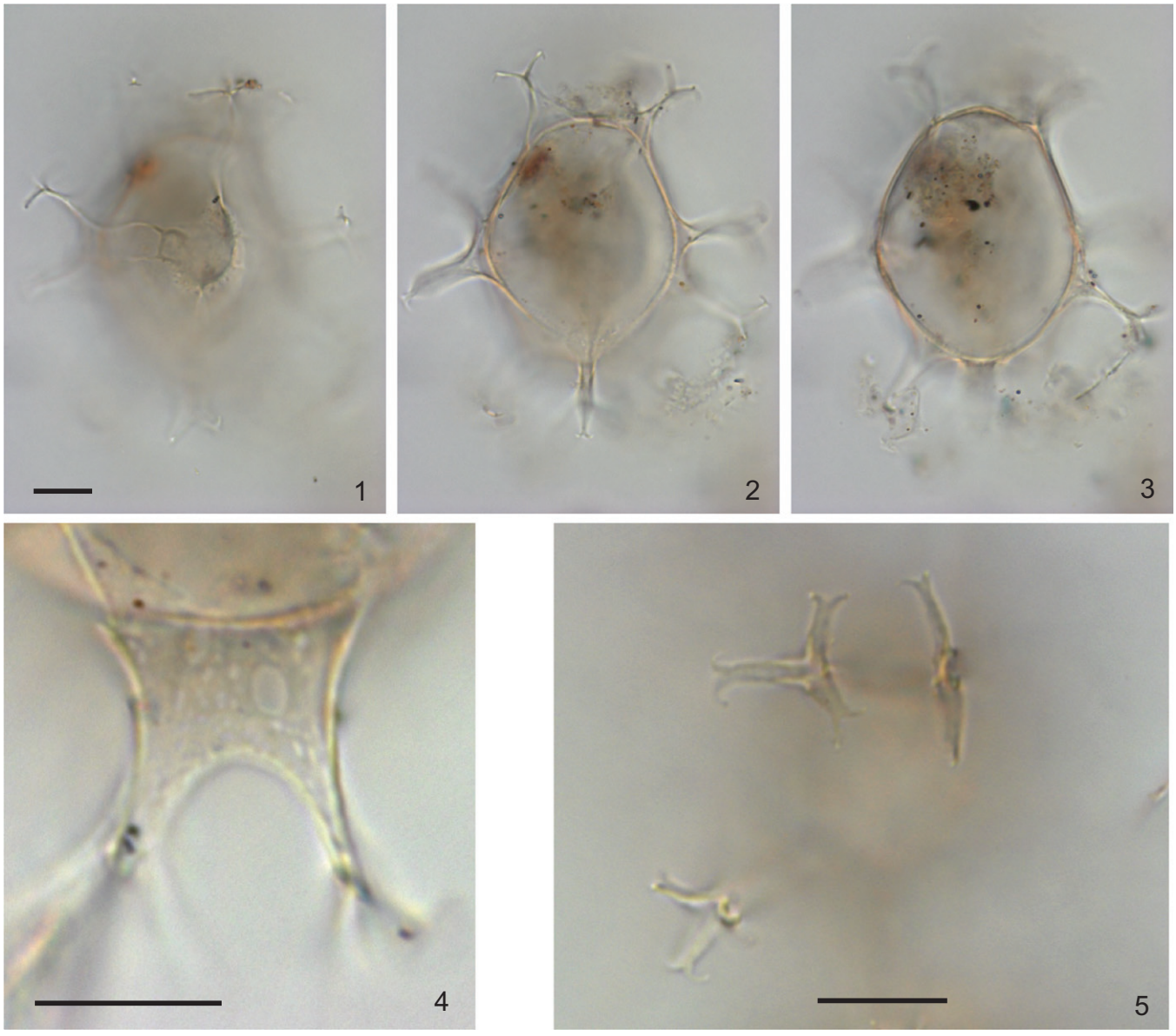

Plate 6. Fig. 1–5: *Spiniferites lazus*. 1–3: Celtic Sea St. 5 4100 cs 9–4, sp. 9; 1–2: High focus, incrementally lowering; 3: Optical section. 4: Celtic Sea St. 5 4100 cs 9–4, sp. 10, detail of perforations at process base; 5: Celtic Sea St. 5 4100 cs 9–4, sp. 2, detail of process terminations. Scale bar =10 μm.

Remarks. New photomicrographs of the holotype are presented in Plate 2. This species was also recorded in the newly processed topotype material from Dee Estuary.

Occurrence. Recorded from (mid) late Miocene or maybe middle Miocene to Recent (Londeix et al. 2018).

Spiniferites lazus Reid 1974
Plate 6, Figures 1–5, Plate 10, Figures 4–8.

Synonymy. None.

Dimensions. Reid (1974) – holotype: test 48 × 33 μm, height processes 14 μm. Range: length test: 44–58 μm, width test: 31–42 μm; depth: 31–39 μm; process length 12–25 μm; girdle width: 5–8 μm. Number of specimens measured: 32. Our measurements on topotype material from the three estuaries in the Irish Sea – length 42 (48) 56 μm; width 30 (37) 44 μm. Number of specimens measured: 4.

Original description (Reid 1974, p. 604). "The test is ovoid in polar view with a thick wall 1–1.5 μ which is made up of two layers of equal thickness. Sutural septae increase in height towards the processes which have process tips like wide petals in plan view. Processes surrounding the apical plates, 3′ and 2′ are in the form of a crown connected by clear fenestrate sutural septae. Girdle processes may be simple or geminal. At the junction of the postcingular and antapical plates stout simple processes are found. They may be geminal along the junction of 4‴, 3‴? A clear geminal process with a high fenestrate flange is found along the junction of 6‴ an [*sic*] 1⁗. Bases of processes are hollow, but do not pass through the test wall. A clear node or boss is found at the junction of plates 3′, 2′ and 1′. Plate 1′ and 4′ appear to be combined as there is no evidence for a suture separating them. The sulcus is slightly sigmoidal, of moderate width and with no clear sulcal plates. Tabulation is typical for the genus 3′?, 0a, 6″, 6g, 5–6″, 1P and 1⁗. The archeopyle is dorsal, precingular 3″ and reduced with a distinct elongate bell shape."

Additional observations. The central body is elongated, ovoid, with an asymmetrical epi- and hypocyst, sometimes

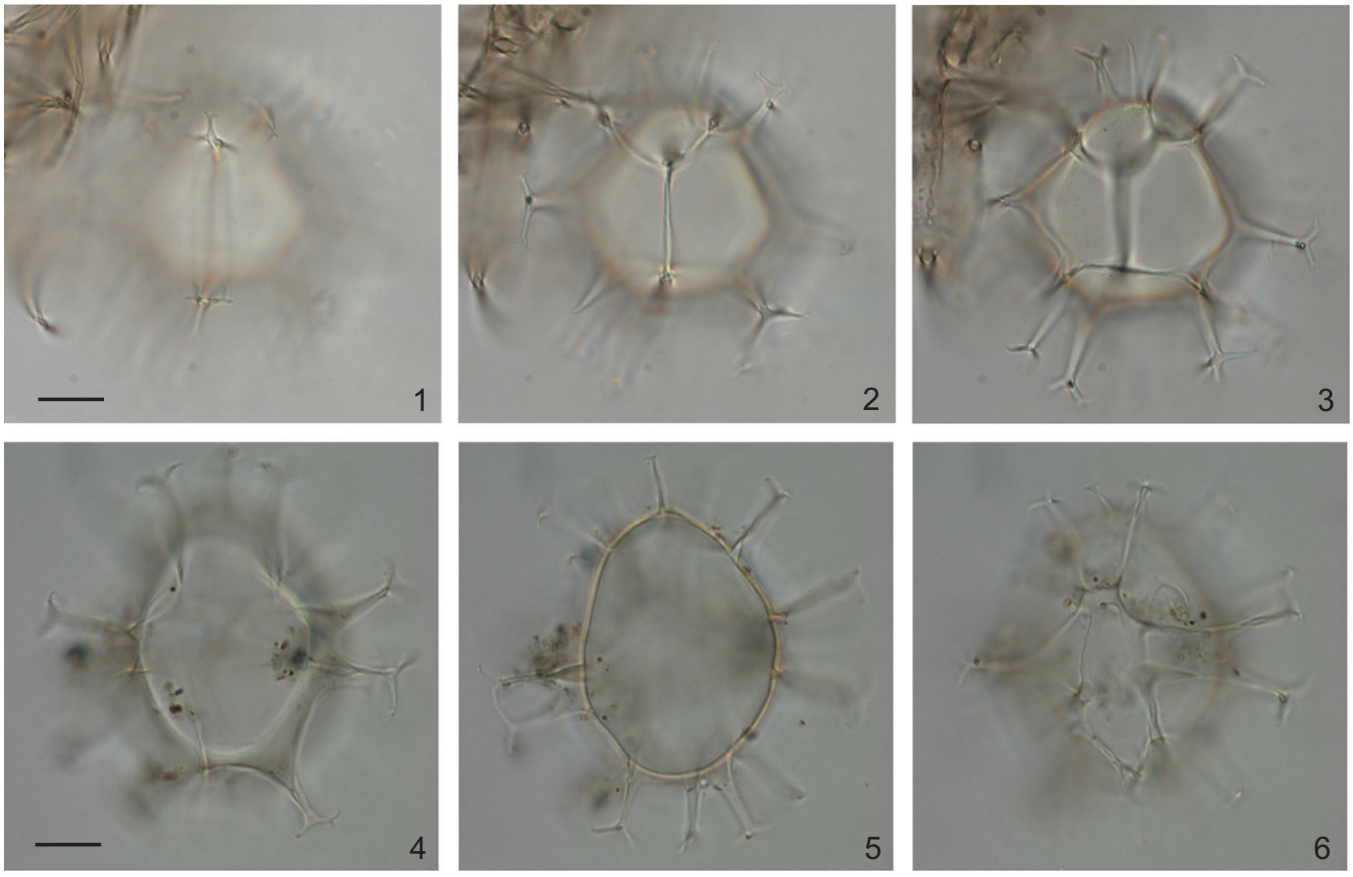

Plate 7. 1–6: *Spiniferites ramosus*. 1–3: Dee Estuary 3/3; incrementally lowering focus. 4–6: Celtic Sea St. 5 4100 cs 9–4; 5: high focus; 6: optical section; 7: low focus. Scale bar =10 μm. [Mismatch]

with a faint apical boss (Plate 6, Figure 3). The wall is thick (1.2 μm) and the surface is microgranular to microreticulate (Plate 10, Fig. 8). The processes are exclusively gonal and have fenestrate bases (Plate 6, Figure 4). The distal ends on processes of *Spiniferites lazus* are typically without fenestrations, trifurcate with elongated furcations ending in short bifurcate tips (Plate 6, Figure 5). The intergonal processes, as described by Reid (1974), were not observed in cysts from the topotype material. The girdle is displaced by four times its width. The archeopyle corresponds to plate 3″ and is reduced.

Remarks. Cysts attributable to this species were recorded in the topotype material from Dee Estuary, Conwy Marina and Caernarvon.

Comparison. The fenestrate process bases are the most typical characteristic of *Spiniferites lazus*, although fenestrate bases have also been observed on *Spiniferites bentorii* and *Spiniferites hainanensis* Sun and Song 1992. *Spiniferites bentorii* is easily recognized by the pear-shaped ambitus of the central body, whereas *Spiniferites hainanensis* has a smaller number of fenestrations on the processes, while perforations are also present on the sutural crests. *Spiniferites hainanensis* furthermore has intergonal processes (Sun and Song 1992). *Spiniferites septentrionalis* has large fenestrations in the distal ends of its processes.

Occurrence. Middle Miocene (?) to Recent (Londeix et al. 2018).

Spiniferites ramosus (Ehrenberg 1837) Mantell 1854 sensu Rochon et al. 1999
Plate 7, Figures 1–7.

Synonymy. *Spiniferites bulloideus* (Deflandre and Cookson 1955) Sarjeant 1970 sensu Reid 1974, Plate 2, figures 17–19. *Spiniferites ramosus* (Ehrenberg 1838) Mantell 1854 sensu Harland 1977, Plate 1, Figures 5, 6; Rochon et al. 1999, Plate 9, Figures 4–6. non *Spiniferites ramosus* var. *ramosus* sensu Davey and Rogers 1975 (Plate 1, Fig. 5).

Original description (Reid 1974, p. 600). "The test is oval in equatorial view, and circular to semi-circular in other views. The epitract narrowing towards the apex frequently has a shoulder at the junction of the precingular and apical plates. A thin 1μ, two layered wall with a smooth surface is ornamented with low sutural septae forming gonal processes. The processes are simple, relatively long with trifurcations that may be up to half the length of the process and have clear bifid tips. Combined geminal processes delimit the boundaries of the girdle fields and a complicated process may be found at the head of the sulcus. The junction of plates 4‴ and 1⁗ is marked by a germinal process which may at times be strongly developed and have two columnar stems expanding into a 'trumpet' shape at the distal tips. If suitably orientated the apex shows an apical horn. Girdle spiral, displaced by its own width. The girdle appears relatively wider in the smaller forms of this species. Sulcus relatively wide, showing signs of platelets. Plate 1′, 4′ appear to be fused into one plat [*sic*]. Plate 1‴ is relatively short in length and wide laterally. Plate 6″ is a narrow elongate triangle. Tabulation as for the genus. Archeopyle dorsal precingular 3″.

Additional observations. The specimens we observed conform to those described by Reid (1974) in having exclusively gonal processes, smooth walls and low sutural crests.

Remarks. See Mertens et al. (2018) for the taxonomic history.

Spiniferites membranaceus (Rossignol 1964) Sarjeant 1970
Plate 8, Figures 1–6.

Synonymy. *Hystrichosphaera furcata* var. *membranacea* Rossignol 1964; *Hystrichosphaera ramosa* var. *membranacea* (Rossignol 1964) Davey and Williams 1966; *Hystrichosphaera membranacea* (Rossignol 1964) Wall 1967.

Dimensions. Reid (1974) – Test 34×34 to 44×43 μm. Height of the antapical flange 2–21 μm. Process height 12–17 μm. Girdle width 5–8 μm. Number of specimens measured: 16. Our measurements – length 36 (41.4) 44 μm, width 34.4 (38.1) 42 μm, antapical flange height 12 (14) 16 μm, process height 12 (12.3) 12.8 μm. Number of specimens measured: 5.

Original description (Reid 1974, p. 605). "The test is circular to ovoid and slightly elongate in a posterior-anterior direction, with an apex that is marked by a clear boss. The girdle is inclined and displaced by twice its width and the sulcus is slightly sigmoid, moderately wide and consists of plates AS, RA, RS, LS and PS. The tabulation and plate pattern is typical for the genus with four apical plates and a dorsal, reduced, precingular archeopyle. The wall is two layered, each layer of equal thickness, with a microgranular to micropunctate surface ornament. Two high processes are found at the angular junctions of plates 1′′′′ and 4′′′. They are joined by an equally high membranous flange along the junction of these two plates. A sutural geminal process is found between plates 6′′′ and 1′′′′. Junctions between cingular plates are marked by similar narrow geminal processes. Plate 1P is surrounded by a more complex crown of processes joined by high septae. Apical plates are delimited from the precingulars by a crown of processes connected by membranous sutural septae. Other processes are gonal and simple. A plan view of the process tips shows narrow trifurcations from a central axis with Y-shaped terminations."

Additional observations. Processes are exclusively gonal. Specimens with broken or reduced processes were often observed, lacking furcations on the distal ends (Plate 8, Figs. 1–2). The base of the sutural crests is typically observed as an undulating double line (Plate 8, Fig. 1). The cyst wall and processes are granular. The cingular displacement of two times its own width is illustrated in Plate 8, Fig. 2, which also shows a view of the slightly sigmoid sulcal area.

Remarks. Wall et al. (1977) remarked that *Spiniferites membranaceus* sensu Reid (1974) is probably not conspecific with that of Rossignol (1964), an observation repeated by Harland (1983). Having not been able to observe specimens from Rossignol (1964), we were not able to confirm this observation.

Spiniferites mirabilis (Rossignol 1964) Sarjeant 1970
Plate 8, Figures 7–9.

Synonymy. *Hystrichosphaera mirabilis* Rossignol 1964 [the species was first invalidly described by Rossignol (1962, p. 132, without any images), because no holotype was designated]. *Spiniferites splendidus* Harland 1979, p. 537, plate 3, figures 1–2 by Limoges et al. (2018).

Dimensions. Reid (1974) – Test 44×48 to 58×60 μ. Maximum process height 15–21 μ. Girdle width 6–8 μ. Number of specimens measured: 16. Our measurements – length 40 (47.6) 60 μm, width 36 (40) 46 μm, process length 10.4 (13.9) 18 μm. Number of specimens measured: 5.

Original description (Reid 1974, p. 606). "Oval, slightly elongated cysts that are circular in polar view. The antapical area is ornamented by processes that are connected by a high sutural flange along the junction of plates 1′′′′ and 4′′′. At the junction of these two plates with 3′′′ and 5′′′ large processes emerge from the flange. Stout, rigid hollow gonal and sutural processes ornament the remainder of the test. The wall is thin, two layered and frequently ruptured or folded with a distinct microgranular surface. The sinistral girdle is displaced by three times its width ventrally, and the sulcus is relatively wide and shows the following plates clearly, PS, IS, LS, RS? Sutures between the right accessory and anterior sulcal plates were not seen. Tabulation is typical for the genus with a long, narrow plate 1′′′ which is delimited by low granular connections between the processes. The archeopyle is dorsal, precingular 3′′, quadrangular with rounded corners."

Additional observations. Our specimens conform to the specimens described by Reid (1974).

Remarks. This species was observed in the Conwy Marina, Dee and Caenarvon estaries.

Genus *Achomosphaera* Evitt 1963

Achomosphaera ramosasimilis (Yun 1981) Londeix et al. 1999
Plate 8, Figures 10–12.

Synonymy. *Achomosphaera ramulifera* subsp. *ramosasimilis* Yun Hyesu 1981. "*Spiniferites ramuliferus*" sensu Reid 1974 according to Londeix et al. (2018)

Dimensions. Reid (1974) – Range: 38×50 to 33×42 μ; Process length, Apical 12–17 μ, Cingular 17–25 μ, Antapical 17–25 μ. Number of specimens measured: 15. Our measurements – length 43.0 (43.8) 44.9, width 34.6 (34.9) 37.4, process length 13.3 (14.9) 16.7, wall thickness 0.7 (1.1) 1.6. Number specimens measured: 3.

Original description (Reid 1974, p. 609). "Recent specimens of this species have a distinct rhomboidal shape in equatorial view and ellipsoidal shape in other orientations, agreeing with Deflandre's description of the type material. The test wall is microgranular, two layered and 1 μ thick. Hollow, wide based, sturdy, gonal spines ornament the surface reflecting a tabulation of 3–4′, 6′′, 6C, 5′′′, 0–1P′′′′. At the junction of plates 1′′′′ and 4′′′ two large processes are joined together at their bases to form a low flange. Cingular processes may also be joined together at their bases but are slender with a much shorter base. The processes are trifurcate at their distal end with the trifurcations parallel to the test wall. The processes may divide into two, each division then trifurcating to the slender extreme tips, which have a short Y-shaped bifurcation. The apex has a distinct process with two short extensions projecting from the distal end as

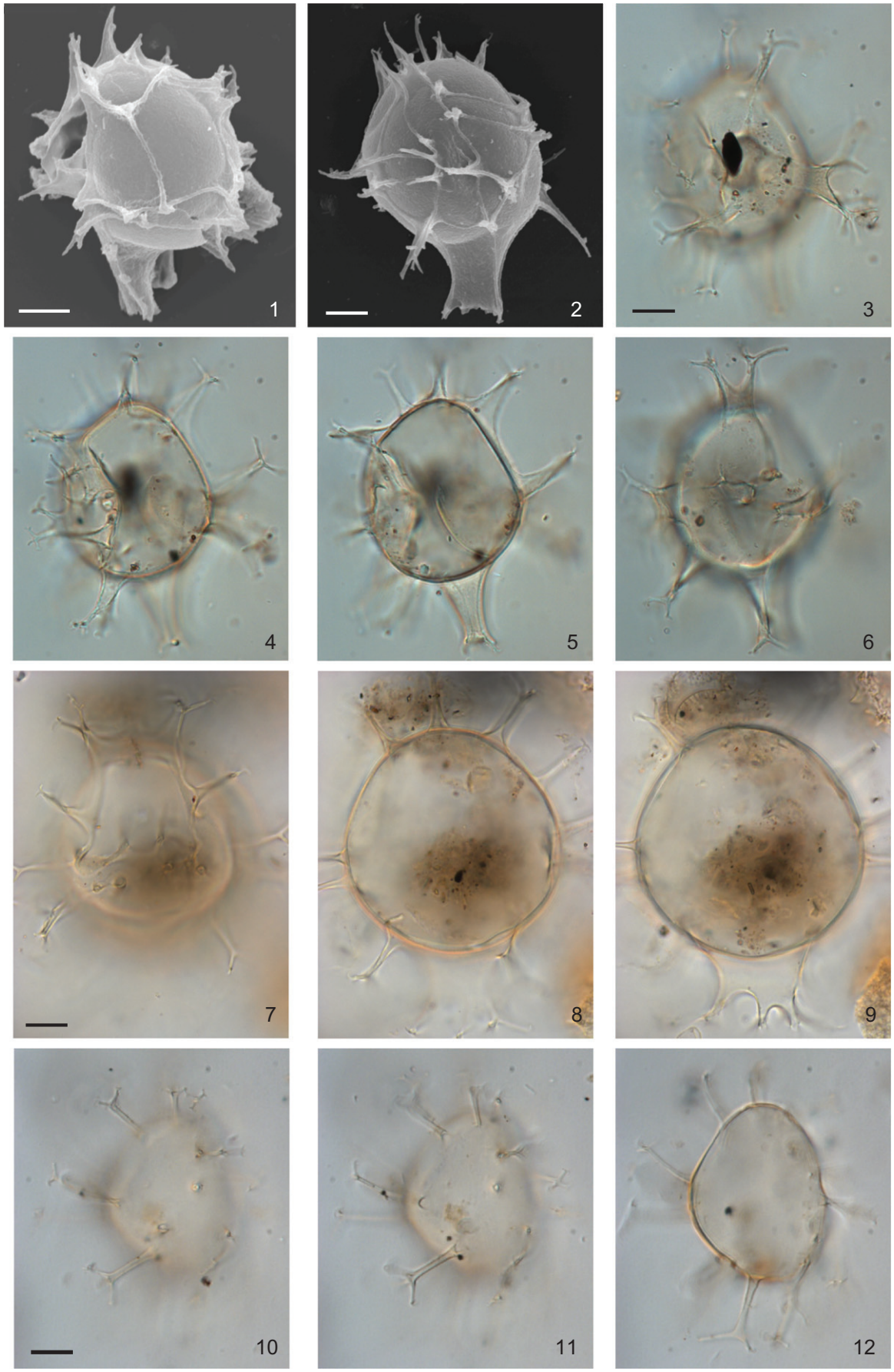

Plate 8. 1–6: *Spiniferites membranaceus*. 1–2. Dee Estuary, SEM-images. 3–6: Celtic Sea St. 6 3100 cs 8–4, 3–4, high focus, 5 optical section, 6 low focus. 7–9: *Spiniferites mirabilis*. Celtic Sea St. 6 4100 cs 9–3. 7: high focus; 8: optical section; 9: low focus. 10–12: *Achomosphaera ramosasimilis*. Verrebroek dock section. Incrementally lowering focus. Scale bar =10 μm.

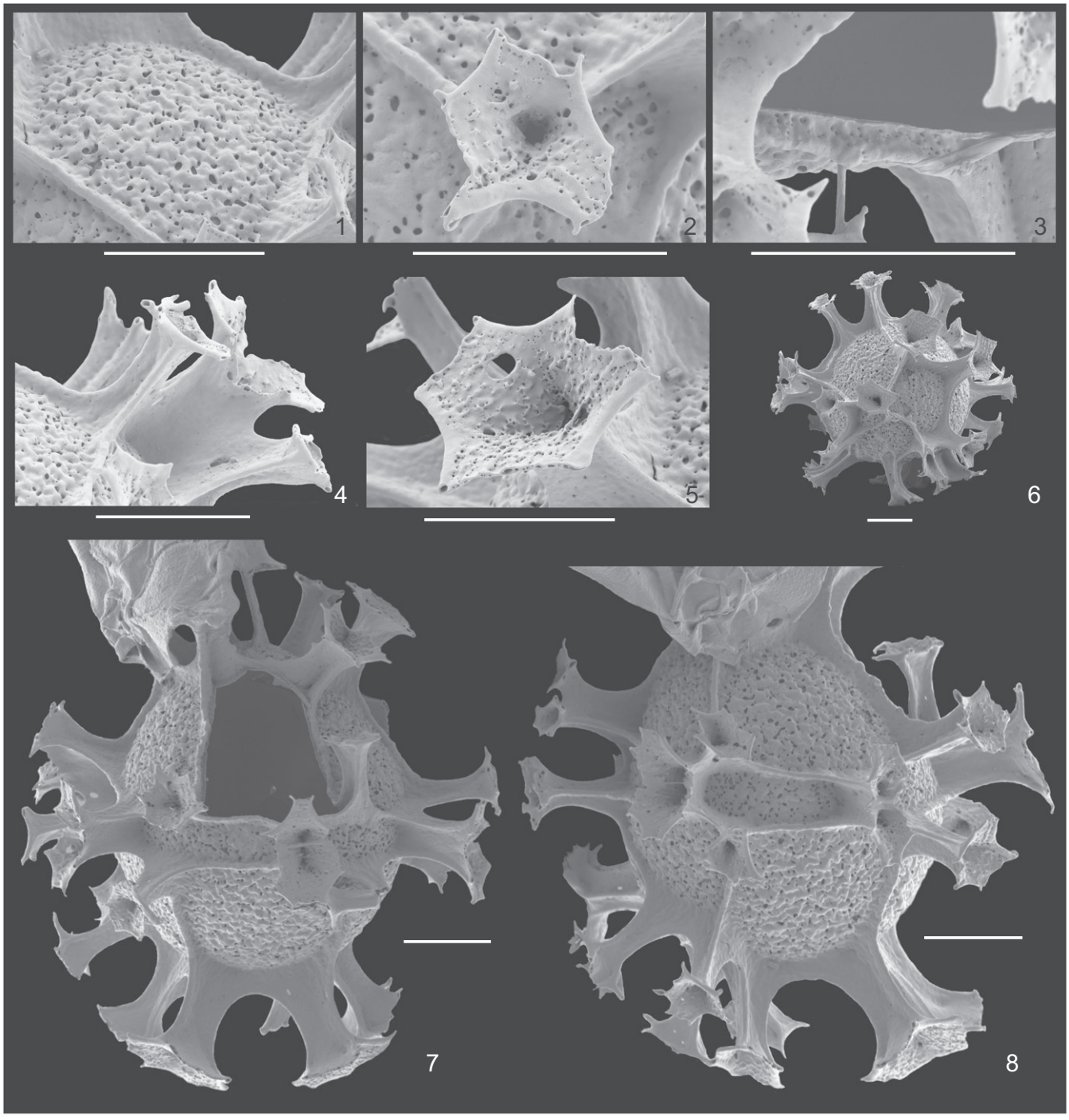

Plate 9. 1–8: *Spiniferites ristingensis*. Britanny, Vilaine Estuary. 1: detail of external wall texture; 2: axial detail of process termination; 3: detail of wall at the archeopyle margin; 4: detail of cingular processes; 5: oblique view of process termination; 6: antapical view; 7: dorsal view; 8: lateral view. Scale bar =10 μm.

well as the bifurcating tips. The processes appear to extend through the endophragm but are not open to the interior. Their base is covered by a thin membrane. A precingular apical-antapically elongated archeopyle is formed by the loss of plate 3″."

Additional observations. Our specimens conform to the specimens described by Reid (1974). The specimens are close to the description of *Spiniferites ramosus* sensu Rochon et al. (1999), but have no sutural traces, and narrower process bases.

Remarks. Reid (1974, p. 609) did not accept the genus *Achomosphaera* and considered his specimens to belong to the genus *Spiniferites*, although he mentioned the absence of sutural traces. Here, however, we assign these specimens to the genus *Achomosphaera*. The species differs from *Achomosphaera andalousiense* and *Spiniferites septentrionalis* in having no fenestrate distal ends on the processes.

Occurrence. We did not observe this species in the topotype material from the British estuaries. However, we encountered specimens that conform to Reid's (1974) description of *Spiniferites ramuliferus* in type material of *Spiniferites conicon-cavus* from the Pliocene Verrebroek section of Belgium (De Schepper et al. 2004). Since Reid (1974) did not depict

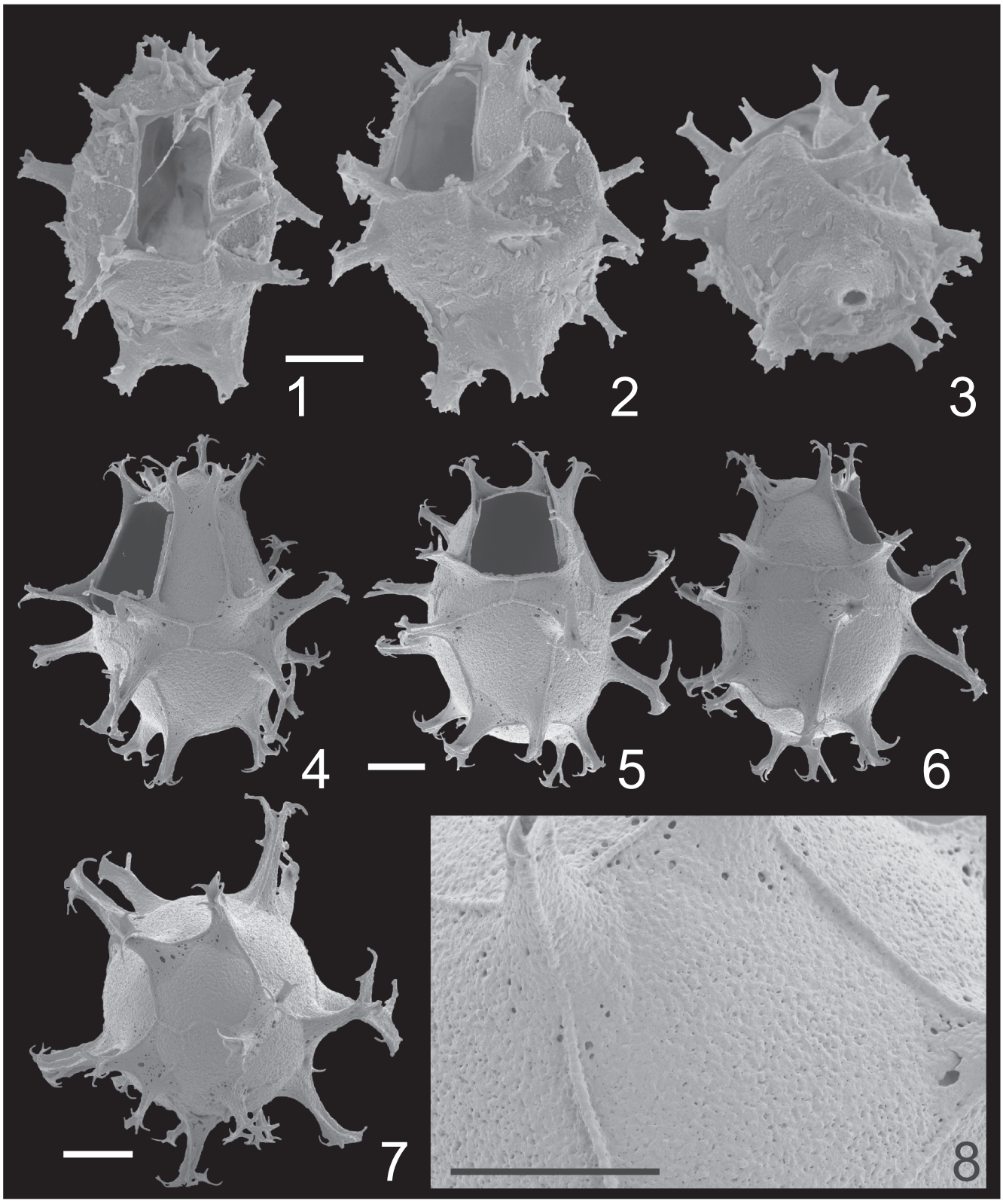

Plate 10. 1–3: *Spiniferites coniconcavus*. Pliocene Verrebroek section, Belgium. 1: antapical view; 2: dorsal view on archeopyle; 3: oblique dorsal view on archeopyle. 4–8: *Spiniferites lazus*. 4: right lateral view; 5: dorsal view with archeopyle visible; 6: left lateral view; 7: antapical view; 8: detail of wall surface. Scale bar =10 μm, except in 8, where it is 2 μm.

specimens with cell content we cannot evaluate whether these specimens are reworked, and, as such, whether or not this genus is extant.

4. Cyst wall composition

Three *Spiniferites* species originally described in Reid 1974 (*Spiniferites belerius*, *Spiniferites elongatus* and *Spiniferites*

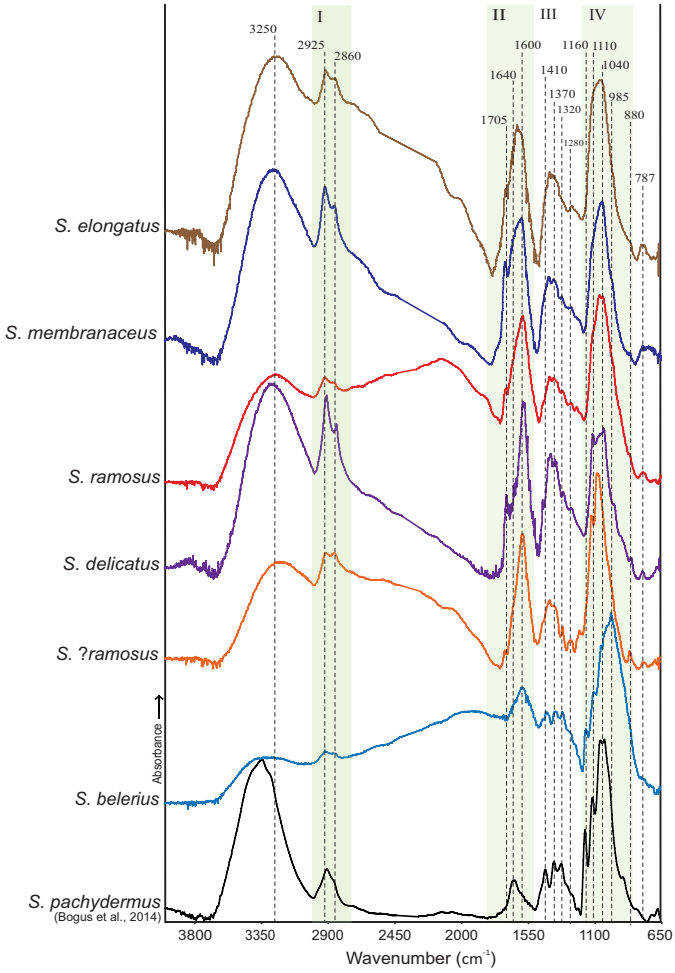

Figure 2. FTIR spectra of morphologically identifiable *Spiniferites* species from Dee estuary sediments. The spectrum colors correspond to Figure 3. IR band regions used in the relative strength comparison are (I) 3010–2775 cm^{-1}, (II) 1850–1500 cm^{-1}, (III) 1500–1185 cm^{-1}, and (IV) 1185–860 cm^{-1}. The published spectrum of *Spiniferites pachydermus* (core GeoB4804, Benguela upwelling region) is shown for comparison (Bogus et al. 2014).

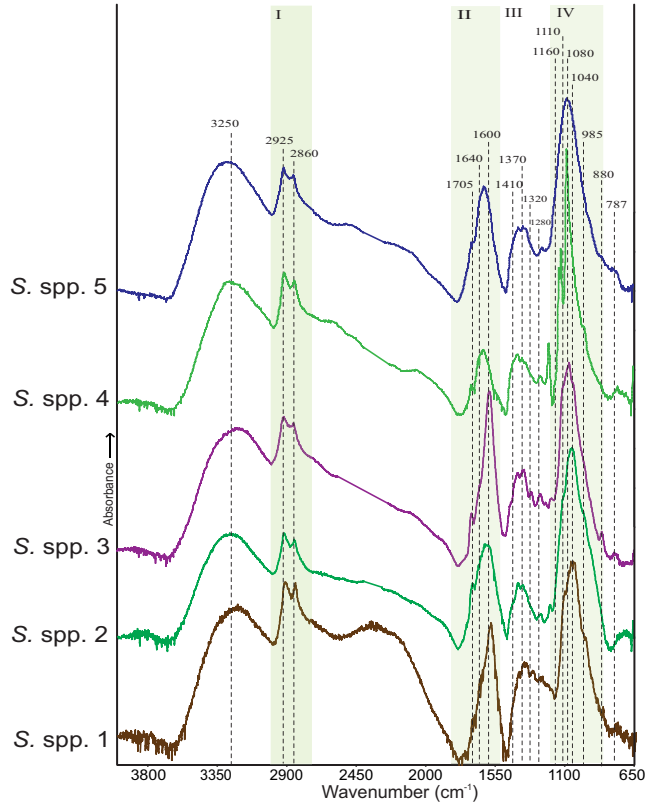

Figure 3. FTIR spectra of morphologically unidentifiable species of the genus *Spiniferites* (*Spiniferites* spp.) from Dee estuary sediments. The spectrum colors correspond to Figure 3. IR band regions used in the relative strength comparison are (I) 3010–2775 cm^{-1}, (II) 1850–1500 cm^{-1}, (III) 1500–1185 cm^{-1}, and (IV) 1185–860 cm^{-1}.

delicatus) were measured for their cyst wall composition after isolation from Dee Estuary sediments (Figure 2). Additional species recorded by Reid in the Dee estuary sediments were also analyzed, including *Spiniferites membranaceus*, *Spiniferites? ramosus* and *Spiniferites ramosus*, and compared with the only published spectrum of a *Spiniferites* species (*Spiniferites pachydermus* from the Benguela upwelling region; Bogus et al. 2014) (Figure 2). Five other morphologically unclassified species of *Spiniferites* were recorded and analyzed (Figure 3). In all cases, a single specimen was analyzed. As such, intraspecific variability was not assessed. However, it is expected that specimens of the same species will show similar spectra if they come from the same locality, as was demonstrated in previous studies (e.g., Mertens et al. 2015a).

All of the cyst walls are composed of a complex biopolymer, likely carbohydrate-based, that is broadly consistent with other published spectra from the same order (Gonyaulacales) (Bogus et al. 2014, Mertens et al. 2015b). Due to the complexity of the biopolymer it was not possible to definitively assign each of the IR bands. However, the differences in the intensity and position of bands in the cyst walls of the different *Spiniferites* species reflect more general variability in dinosporin composition (Figure 4).

For all specimens (Figures 2 and 3), the region between 3600–3000 cm^{-1} showed a broad absorption with a maximum ~3250 cm^{-1} (OH stretch). Absorptions in the 3000–2775 cm^{-1} region (CH stretching; IR band region I) were characterized by two IR bands at 2925 cm^{-1} and 2860 cm^{-1}. These absorptions are present in all specimens and reflect the contribution of CH_2 and CH_3 groups. The related absorptions at 1420 cm^{-1} and 1370 cm^{-1} (CH bending; IR band region III) are also present in all spectra. Additional weaker absorptions in IR band region III (e.g., 1320 cm^{-1} and 1280 cm^{-1}) likely reflect C-OH deformation and C-O stretching. Absorptions between 1850–1500 cm^{-1} (IR band region II) are characteristic of C = C (1600 cm^{-1}) and C = O (1705 cm^{-1} and 1640 cm^{-1}) stretching, and are variable in both their presence and strength between the specimens. For example, the absorption at 1705 cm^{-1} is absent in the spectrum of *Spiniferites belerius*, but this IR band region contains the strongest absorption (1600 cm^{-1}) in the entire spectrum of *Spiniferites delicatus* (Fig. 2), which influences its position in Figure 4. The absorptions between 1185–1030 cm^{-1} (IR band region IV) represent C-O stretching and the deformation vibrations of sugar rings at 1160 cm^{-1} (C-O-C asymmetric vibration), 1110 cm^{-1} (glucose ring stretching), 1080, 1060, 1040 and/or 1030 cm^{-1} (C-O stretching), as well as skeletal ring vibrations and the anomeric region (900–650 cm^{-1}). The series of absorptions in IR band

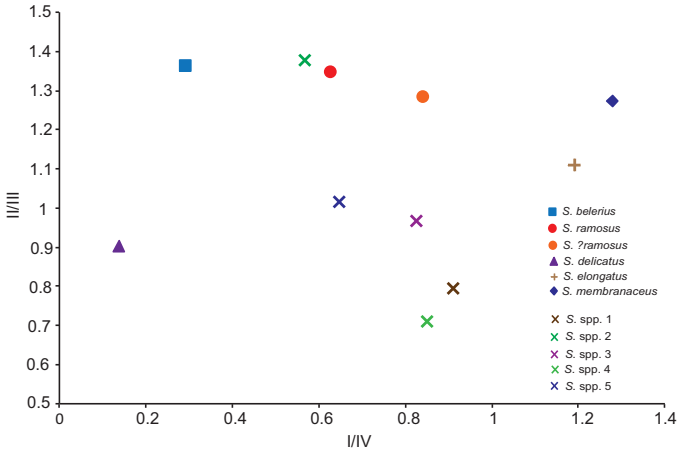

Figure 4. Relative IR band comparison between morphologically identifiable *Spiniferites* species, and morphologically unidentifiable cysts of the genus *Spiniferites*. The IR regions correspond to (I) 3010–2775 cm^{-1}, (II) 1850–1500 cm^{-1}, (III) 1500–1185 cm^{-1}, and (IV) 1185–860 cm^{-1}.

region IV provide a strong argument that a carbohydrate, probably with a β-glycosidic linkage (Pandey 1999; Kačuráková and Wilson 2001), forms the backbone of *Spiniferites* dinosporins, consistent with previous data for species from the order Gonyaulacales (Versteegh et al. 2012; Bogus et al. 2014; Mertens et al. 2015b).

However, there is variability in IR band region IV, particularly with regards to the position of the strongest peak. Only *Spiniferites pachydermus* exhibited the absorption pattern that most closely resembles cellulose (Pandey 1999); none of the Dee Estuary *Spiniferites* specimens had their strongest absorption at 1030 cm^{-1} (Figure 2). The majority of the specimens that could be speciated (*Spiniferites elongatus*, *Spiniferites membranaceus*, *Spiniferites ramosus*, and *Spiniferites delicatus*) exhibited the strongest peak at 1040 cm^{-1} and a second peak at 1110 cm^{-1}. The cyst wall of *Spiniferites belerius* is the most unique in region IV in that the strongest peak is centered at 985 cm^{-1}, but with subsequent peaks at 1040, 1110 and 1160 cm^{-1}, similar to *Spiniferites pachydermus*; it is the only specimen that contains such a shifted primary absorption, and an overall broader series of absorptions, which is reflected in its position in Figure 4. The only other specimen with a dominant absorption in region IV not centered at 1040 cm^{-1} is *Spiniferites? ramosus*, where it is instead centered at 1080 cm^{-1}. This is more similar to many of the unspeciated *Spiniferites* specimens (i.e., *Spiniferites* spp. 3, 4, and 5; Fig. 3) that also exhibit their strongest absorption at 1080 cm^{-1}. *Spiniferites* spp. 1 and 2 exhibit the dominant absorption at 1040 cm^{-1}, which is more in line with the speciated specimens.

All species measured from the topotype material have a more pronounced peak in the range of 1600-1705 cm^{-1} (region II) compared with the spectrum of *Spiniferites pachydermus* from the Benguela upwelling region. This is probably due to environmental differences between the surface waters of the two regions. It has been shown for other species that different water mass conditions lead to different cyst wall chemistries (Mertens et al. 2015a). An analytical factor cannot be fully ruled out, however, although limited published data using a chitin standard (described in Bogus et al. 2014) comparing spectra produced in the respective laboratories demonstrated that the spectra were comparable.

It is clear from both the morphological examination and chemical analysis that *Spiniferites delicatus*, *Spiniferites belerius*, and *Spiniferites membranaceus* are quite distinct (Plates 3, 4 and 8, Fig. 4). The chemical composition of *Spiniferites elongatus* suggests that it is most similar to *Spiniferites membranaceus*, and that *Spiniferites ramosus* and *Spiniferites? ramosus* are most similar to each other (Fig. 4). In conjunction with the morphological determination for *Spiniferites ramosus* and *Spiniferites? ramosus*, it is possible that they are, in fact, the same species (*Spiniferites ramosus*); unfortunately, it is not currently possible to be conclusive regarding this.

If the visually defined species' cyst wall chemistries are used as a guide, there is some indication that dinosporin composition can constrain the unspeciated *Spiniferites* specimens. This is particularly evident for *S.* spp. 2, as it plots very close to *Spiniferites ramosus* and close to *Spiniferites? ramosus*, suggesting that this specimen may not be a different species, and that the difficulty of its morphological classification is caused by the wide range in morphological variability. However, the other unspeciated *Spiniferites* specimens seem to cluster nearer to each other with *Spiniferites* spp. 4 and 1 and *Spiniferites* spp. 3 and 5 showing greater proximity (Fig. 4). This could indicate that each of these couples is a different species, or that all four represent morphological variations of the same species. It is currently not possible to determine this, but it is clear that their dinosporins are different from the speciated *Spiniferites*. The cyst wall chemistry also demonstrates the ambiguity in defining species of this genus.

5. Conclusions

The *Spiniferites* species described by Reid (1974), *Spiniferites belerius*, *Spiniferites delicatus*, *Spiniferites elongatus* and *Spiniferites lazus*, were re-studied to improve their morphological descriptions and iconography. The holotypes of *Spiniferites delicatus* and *Spiniferites elongatus* were re-photographed to improve the image resolution. Both of the latter species, together with *Spiniferites belerius* and *Spiniferites lazus*, were also recorded in newly processed topotype material from three British estuaries (Dee, Conwy Marina and Caernarvon). *Spiniferites belerius* is characterized by its size and the trumpet-shaped process, and its position has been assessed as the junction of plates 1′′′′ and 1p. *Spiniferites delicatus* was well-defined in the original description but the distinction with *Spiniferites ristingensis* needs further investigation. Specimens of *Spiniferites elongatus* and *Spiniferites lazus* posed no problems with the original descriptions.

Specimens of *Spiniferites membranaceus*, *Spiniferites mirabilis*, *Spiniferites ramosus* (called *S. bulloideus* by Reid 1974) were also identified in and illustrated from the topotype material from the British estuaries. The species *Spiniferites hyperacanthus* and *Spiniferites pachydermus* were not recorded. *Spiniferites ramuliferus*, now known to be *Achomosphaera ramosasimilis* was not recorded in the topotype samples, but cysts corresponding to the description of

this species as given by Reid (1974) were identified in material from the Pliocene of Belgium.

Along with the taxonomic re-investigation, the cyst wall composition of *Spiniferites* specimens isolated from Dee Estuary sediments, both visually speciated (*Spiniferites belerius*, *Spiniferites ramosus*, *Spiniferites? ramosus*, *Spiniferites delicatus*, *Spiniferites elongatus*, *Spiniferites membranaceus*) and not (*Spiniferites* spp. 1–5), were compared. The results showed variations in the *Spiniferites* species' dinosporin compositions, supporting the suggestion that cyst wall chemistry may be species specific and evident when other factors are controlled (i.e. geography and environmental conditions). The cyst wall chemistries of *Spiniferites delicatus*, *Spiniferites belerius*, and *Spiniferites membranaceus* were the most distinct, suggesting that the morphological assignation for the different species is supported by the cyst wall chemistry. It also provides some impetus for clarifying the species' descriptions for *Spiniferites belerius* and *Spiniferites delicatus* in particular.

The unspeciated *Spiniferites* specimens were mostly difficult to constrain chemically, as they did not show clear overlap with the speciated spectra. Overall, the visually unidentifiable specimens represent examples of the ambiguity in speciating *Spiniferites* specimens morphologically and chemically. However, *Spiniferites* spp. 1, and 3 to 5 clustered nearer to each other in terms of cyst wall chemistry, suggesting that they may be the same species, but with enough morphological variation to make their visual identification difficult. Furthermore, *Spiniferites* spp. 2 plotted very close to *Spiniferites ramosus*, indicating that this specimen may, in fact, be the same species.

Acknowledgements

C. Wellman and P.C. Reid are thanked for permission to consult the holotype material in the University of Sheffield palaeontology collections. The Hercules Foundation (Flanders) is gratefully acknowledged for financial support (FT-IMAGER project AUGE/13/16).

Disclosure statement

No potential conflict of interest was reported by the authors.

Author contributions

PG, KM, KB, FM & SL conceived the study; PG studied and photographed the holotypes in Sheffield; FM provided the sediments from topotype localities; PG processed the new sediment samples; KM & PG studied and photographed the cysts from topotype localities with light microscope; KM & PG processed the residues, picked cysts for FTIR; PG, KM & HV did spectral analysis for cyst wall composition; KB interpreted the spectra and the relation to dinocyst wall chemistry; PG, KM, KB & SL wrote the paper and PG, KM & SL made the plates.

References

Adl SM, Simpson AGB, Farmer MA, Andersen RA, Anderson OR, Barta JR, Bowser SS, Brugerolle G, Fensome RA, Fredericq S, et al. 2005. The new higher level classification of Eukaryotes with emphasis on the taxonomy of Protists. J Eukaryot Microbiol. 52:399–451.

Bogus K, Harding IC, King A, Charles AK, Zonneveld K, Versteegh GJM. 2012. The composition of species of the *Apectodinium* complex (Dinoflagellata). Rev Palaeobot Palynol. 183:21–31.

Bogus K, Mertens KNM, Lauwaert J, Harding IC, Vrielinck H, Zonneveld K, Versteegh GJM. 2014. Differences in the chemical composition of organic-walled dinoflagellate resting cysts from phototrophic and heterotrophic dinoflagellates. J Phycol. 50:254–266.

Cookson IC, Eisenack A. 1974. Mikroplankton aus australischen mesozoischen und tertiären Sedimenten. Palaeontogr Abt B. 148:44–93.

Deflandre G. 1937. Microfossiles des Silex Crétacés. Deuxième Partie. Flagellés incertae sedis. Hystrichosphaeridées - Sarcodinés. Organismes divers. Annales Paléont. 26:51–103.

Deflandre G, Cookson IC. 1955. Fossil microplankton from Australian Late Mesozoic and Tertiary sediments. Aust J Mar Freshw Res. 6:242–313.

De Schepper S, Head MJ, Louwye S. 2004. New dinoflagellate cyst and incertae sedis taxa from the Pliocene of northern Belgium, southern North Sea Basin. J Paleontol. 78:625–644.

Ellegaard M. 2000. Variations in dinoflagellate cyst morphology under conditions of changing salinity during the last 2000 years in the Limfjord, Denmark. Rev Palaeobot Palynol. 109:65–81.

Ellegaard M, Lewis J, Harding IC. 2002. Cyst-theca relationship, life cycle, and effects of temperature and salinity on the cyst morphology of *Gonyaulax baltica* sp. nov. (Dinophyceae) from the Baltic Sea area. J Phycol. 38:775–789.

Fensome RA, Taylor FJR, Norris G, Sarjeant WAS, Wharton DI, Williams GL. 1993. A classification of fossil and living dinoflagellates. New York (NY): American Museum of Natural History (Micropaleontology Special Publication; vol. 7); p. 1–245.

Fensome RA, MacRae RA, Williams GL. 2008. DINOFLAJ2, Version 1. American Association of Stratigraphic Palynologists, Data Series no. 1.

Harland R. 1977. Recent and late Quaternary (Flandrian and Devensian) dinoflagellate cysts from marine continental shelf sediments around the British Isles. Palaeontographica B. 164:87–126.

Harland R. 1983. Distribution maps of recent dinoflagellate cysts in bottom sediments from the North Atlantic Ocean and adjacent seas. Palaeontology. 26:321–387.

Head MJ. 2007. Last Interglacial (Eemian) hydrographic conditions in the southwestern Baltic Sea based on dinoflagellate cysts from Ristinge Klint, Denmark. Geol Mag. 144:987–1013.

Kačuráková M, Wilson RH. 2001. Developments in mid-infrared FT-IR spectroscopy of selected carbohydrates. Carbohydr Polym. 44:291–303.

Kokinos JP, Eglinton TI, Goñi MA, Boon JJ, Martoglio PA, Anderson DM. 1998.Characterization of a highly resistant biomacromolecular material in the cell wall of a marine dinoflagellate resting cyst. Org Geochem. 28:265–288.

Lewis J, Rochon A, Ellegaard M, Mudie PJ, Harding IC. 2001. The cyst-theca relationship of *Bitectatodinium tepikiense* (Dinophyceae). Eur J Phycol. 36:137–146.

Limoges A, Londeix L, Mertens KN, Rochon A, Pospelova V, Cuéllar T, de Vernal A. 2018. Identification key for Pliocene and Quaternary Spiniferites taxa bearing intergonal processes based on observations from estuarine and coastal environments. Palynology. 42(S1). doi:10.1080/01916122.2018.1465733

Lindemann E, 1928. Abteilung Peridineae (Dinoflagellatae). In: Engler A, Prantl, K, editors. Die Naturlichen Pflanzenfamilien nebst ihren Gattungen und wichtigeren Arten insbesondere den Nutz-pflanzen. Zweite stark vermehrte und verbesserte Auflage herausgegeben von A. Engler. 2 Band. Leipzig: Wilhelm Engelmann; p. 3–104.

Londeix L, Zonneveld K, Masure E. 2018. Taxonomy of Quaternary species of Spiniferites and related genera. Palynology. 42(S1). doi:10.1080/01916122.2018.1465740

Mantell GA. 1854. The medals of creation; or first lessons in geology and the study of organic remains. 2nd ed. Vol. 2. London, H.G. Bohn.

Marret F, Scourse J, Austin W. 2004. Holocene shelf-sea seasonal stratification dynamics: a dinoflagellate cyst record from the Celtic Sea, NW European shelf. The Holocene. 14:689–696.

Mertens KN, Ribeiro S, Bouimetarhan I, Caner H, Combourieu-Nebout N, Dale B, de Vernal A, Ellegaard M, Filipova M, Godhe A, et al. 2009. Process length variation in cysts of a dinoflagellate, *Lingulodinium*

machaerophorum, in surface sediments: investigating its potential as salinity proxy. Mar Micropal. 70:54–69.

Mertens KN, Takano Y, Yamaguchi A, Gu H, Bogus K, Kremp A, Bagheri S, Matishov G, Matsuoka K. 2015a. The molecular characterization of the enigmatic dinoflagellate *Kolkwitziella acuta* reveals an affinity to the *Excentrica* section of the genus *Protoperidinium*. Syst Biodivers. 13:509–524.

Mertens KN, Wolny J, Carbonell-Moore C, Bogus K, Ellegaard M, Limoges A, de Vernal A, Gurdebeke P, Omura T, Al-Muftah A, et al. 2015b. Taxonomic re-examination of the toxic armored dinoflagellate *Pyrodinium bahamense* Plate 1906: Can morphology or LSU sequencing separate *P. bahamense* var. *compressum* from var. *bahamense*? Harmful Algae. 41:1–24.

Mertens KN, Gu H, Takano Y, Price AM, Pospelova V, Bogus K, Versteegh GJM, Marret F, Turner RE, Rabalais NN, et al. 2017. The cyst-theca relation of *Trinovantedinium pallidifulvum*, with erection of *Protoperidinium lousianensis* sp. nov. and their phylogenetic position within the Conica group. Palynology. 41:183–202 DOI: 10. 1080/01916122.2016.1147219.

Mertens KN, Van Nieuwenhove N, Gurdebeke PR, Aydin H, Bogus K, Bringué M, Dale B, De Schepper S, de Vernal A, Ellegaard M, et al. 2018. Summary of round table discussions about Spiniferites and Achomosphaera occurring in Pliocene to modern sediments. Palynology. 42(S1). doi:10.1080/01916122.2018.1465739

Olcott Marshall A, Marshall CP. 2015. Vibrational spectroscopy of fossils. Palaeontology. 58:201–211.

Pandey KK. 1999. A study of chemical structure of soft and hardwood and wood polymers by FTIR spectroscopy. J Appl Polym Sci. 71:1969–1975.

Pascher A. 1914. Über Flagellaten und Algen. Berichte der Deutschen Botanischen Gesellschaft. 32:136–160.

Pospelova V, Esenkulova S, Johannessen SC, O'Brien MC, Macdonald RW. 2010. Organic-walled dinoflagellate cyst production, composition and flux from 1996 to 1998 in the central Strait of Georgia (BC, Canada): a sediment trap study. Mar Micropaleontol. 75:17–37.

Reid PC. 1972. The distribution of dinoflagellate cysts, pollen and spores in Recent marine sediments from the coast of the British Isles [dissertation]. Sheffield: University of Sheffield.

Reid PC. 1974. Gonyaulacacean dinoflagellate cysts from the British Isles. Nova Hedwigia. 25:579–637.

Reid PC. 1977. Peridiniacean and Glenodiniacean dinoflagellate cysts from the British Isles. Nova Hedwigia. 29:429–462.

Rossignol M. 1964. Hystrichosphères du Quaternaire en Méditerranée orientale, dans les sédiments Pléistocènes et les boues marines actuelles. Revue de micropaléontologie. 7:83–99.

Sarjeant WAS. 1970. The genus *Spiniferites* Mantell, 1850 (Dinophyceae). Grana. 10:74–78.

Sun X, Song Z. 1992. Quaternary dinoflagellates from arenaceous dolomite in Hainan Island. Acta Micropalaeontologica Sinica. 9:45–52.

Taylor FJR. 1980. On dinoflagellate evolution. BioSystems. 13:65–108.

Van Nieuwenhove N, Potvin E, Heikkilä M, Pospelova V, Mertens KN, Masure E, Kucharska M, Yang EJ, Chomérat N, Zajaczkowski M. 2018. Taxonomic revision of Spiniferites elongatus (the resting stage of Gonyaulax elongata) based on morphological and molecular analyses. Palynology. 42(S1). doi: 10.1080/01916122.2018.1465736

Versteegh GJM, Blokker P, Marshall CP, Pross J. 2007. Macromolecular composition of the dinoflagellate cyst *Thalassiphora pelagica* (Oligocene, SW Germany). Org Geochem. 38:1643–1656.

Versteegh GJM, Blokker P, Bogus K, Harding I C, Lewis J, Oltmanns S, Rochon A, Zonneveld KAF. 2012. Flash pyrolysis and infrared spectroscopy of cultured and sediment derived *Lingulodinium polyedrum* (Dinoflagellata) cyst walls. Org Geochem. 43:92–102.

Wall D, Dale B. 1970. Living hystrichosphaerid dinoflagellate Spores from Bermuda and Puerto Rico. Micropaleontology. 16: 47–58.

Wall, D., Dale, B., Lohmann, G.P., Smith, W.K., 1977. The environmental and climatic distribution of dinoflagellate cysts in modern marine sediments from regions in the north and south Atlantic Oceans and adjacent seas. Mar Micropaleont. 2:121–200.

Zonneveld KAF, Susek E. 2007. Effects of temperature, light and salinity on cyst production and morphology of *Tuberculodinium vancampoae* (the resting cyst of *Pyrophacus steinii*). Rev Palaeobot Palynol. 145:77–88.